Topological energy-function analysis of stability of power systems

K R Padiyar
Department of Electrical Engineering, Indian Institute of
Technology, Kanpur, India

H S Y Sastry
Department of Electrical Engineering, Karnataka Regional
Engineering College, Surathkal, India

*In this paper the direct stability evaluation of power
systems, with voltage-dependent loads, using topological
energy function is given with applications This is based on
the philosophy of a structure-preserving model for power
systems. The loads are modelled as arbitrary functions of
respectively bus voltages. A classical model is assumed for
generators and system equations are formed using centre of
angle (COA) reference. A topological energy function is
developed and applied for the stability evaluation using the
potential-energy boundary surface (PEBS) method.
Examples of a 4-machine and a 7-machine system are con-
sidered for illustration. The critical clearing time (T_{cr}) is
obtained both by digital simulation and by the direct
method for various load characteristics and for different
fault locations.*

*Keywords: short-term system dynamics, transient stability,
Lyapunov method*

I. Introduction

Direct methods for transient-stability analysis are potenti-
ally useful both as off-line tools for planning purposes and
for on-line security assessment[1,2]. Although much research
work has been reported in this area, the application of this
method has been limited by the conservativeness of results,
the computational burden in computing stability regions,
and the use of simple models for generators and loads.
Recent developments such as the use of COA variables, the
concept of controlling unstable equilibrium point (UEP)[3]
and the use of potential-energy boundary surfaces (PEBS)
method[3,4] in evaluating the region of stability, have been
directed at removing some of these limitations.

Hitherto, loads, in general, have been modelled as constant
impedances. This results in a linear network which can be
reduced to a network retaining only the generator internal
buses. This approach has been used for no better reason
than to avoid the nonlinear algebraic equations that result
from the nonlinear voltage-dependent loads. Unfortunately,
this simplification introduces the problem of transfer con-
ductances. In the early investigations, transfer conductances
were entirely neglected or taken into account using
approximation[3,4].

A structure-preserving model for power systems proposed
recently by Bergen and Hill[5] not only eliminates the prob-
lem of transfer conductances but is also advantageous from
the viewpoint of real-time dynamic security assessment and
for incorporating the load characteristics accurately. They
have considered PV-type load buses; however, their assump-
tion of constant bus voltages is not valid, particularly
during the transient caused by a fault. An improvement in
the load models is presented in References 6 and 7. While
in Reference 6 PQ-type load buses (with constant active
and reactive power) are considered, in Reference 7
voltage-dependent reactive power loads are considered
along with constant active power loads

In this paper, a topological energy function is developed
and the stability evaluation is extended to accommodate
the system with arbitrarily specified voltage-dependent
loads. The system equations are formulated using COA
reference and the critical energy is determined using PEBS
method[4]. The computation of faulted trajectory requires
iterative solution of network equations in the presence of
nonlinear loads An algorithm given in Reference 8 is used
for this purpose.

The method is illustrated using 4-machine and a 7-machine
system examples. The critical clearing times obtained by
direct method are compared with those obtained from

digital simulation, for various load characteristics and for different fault locations.

II. Notation

M_i inertia constant of machine i
ω_i angular velocity in COA reference
θ_i, ϕ_i machine and bus angles with respect to COA
E_i internal voltage of machine i
V_i voltage at bus i
P_{mi} mechanical power input to machine i
P_{ei} electrical power generated by machine i
P_{li}, Q_{li} load active and reactive power at bus i
W energy function
M_T $\Sigma_{i=1}^m M_i$

Subscript '0' indicates the quantities evaluated at the stable equilibrium point.

III. System equations

III.1 Dynamic equations of machines

Consider an n-bus multimachine system having m machines supplying nonlinear voltage-dependent loads. In the direct transient-stability evaluation using energy-type Lyapunov functions, the following assumptions are usually made.

1 Each synchronous machine is represented by a classical model, namely, a constant voltage source behind transient reactance.

2 Governor action is not taken into account and thus the mechanical torque is assumed to be constant.

3 Damping coefficients are neglected.

4 Transmission lines are assumed to be lossless. This is generally true as the extra high voltage lines in a power system have high X/R ratio.

The last two assumptions can be relaxed without unduly complicating the analysis. However, these assumptions will lead to the system being conservative, as shown later.

Under the above assumptions, the motion of the ith machine is described by the following differential equations[3] (in COA reference).

$$M_i \dot{\omega}_i = P_{mi} - P_{ei} - \frac{M_i}{M_T} P_{COA} \qquad (1)$$

$$\dot{\theta}_i = \omega_i \qquad (2)$$

where

$$P_{ei} = \frac{E_i V_i \sin(\theta_i - \phi_i)}{x'_{di}} \qquad (3)$$

$$M_T = \sum_{i=1}^m M_i, \quad P_{COA} = \sum_{i=1}^m (P_{mi} - P_{ei}) \qquad (4)$$

In view of the definitions of COA variables[3], we have

$$\sum_{i=1}^m M_i \theta_i = 0 \quad \text{and} \quad \sum_{i=1}^m M_i \omega_i = 0 \qquad (5)$$

III.2 Load model

In the load model considered here, both active and reactive powers are assumed to be arbitrary functions of respective bus voltages. Thus the equations for system loads can be written as

$$P_{li} = f_{pi}(V_i) \qquad (6)$$

and

$$Q_{li} = f_{qi}(V_i), \quad i = 1, 2, \ldots, n \qquad (7)$$

III.3 Power flow equations

For a lossless transmission system, the following equations are applicable

Let

$$g_{1i} = \frac{E_i V_i \sin(\phi_i - \theta_i)}{x'_{di}}, \qquad g_{2i} = \sum_{j=1}^n V_i V_j B_{ij} \sin \phi_{ij}$$

$$g_{3i} = \frac{V_i^2 - E_i V_i \cos(\theta_i - \phi_i)}{x'_{di}}, \qquad g_{4i} = \sum_{j=1}^n V_i V_j B_{ij} \cos \phi_{ij}$$

The active power injected into the network from bus i is

$$P_i = g_{1i} + g_{2i}, \quad \text{for } i = 1, 2, \ldots, m \qquad (8)$$

$$= g_{2i}, \quad \text{for } i = m+1, m+2, \ldots, n \qquad (9)$$

The reactive power injection at bus i is

$$Q_i = g_{3i} + g_{4i}, \quad \text{for } i = 1, 2, \ldots, m \qquad (10)$$

$$= g_{4i}, \quad \text{for } i = m+1, m+2, \ldots, n \qquad (11)$$

In the above expressions, $B_{ij} = \text{Im}\,[\mathbf{Y}_{bus}(i,j)]$, where $\mathbf{Y}_{bus}$ is the admittance matrix of the network (without including the machine reactances).

The power flow equations at bus i can be written as

$$P_i + P_{li} = P_i + f_{pi}(V_i) = 0 \qquad (12)$$

and

$$Q_i + Q_{li} = Q_i + f_{qi}(V_i) = 0, \quad \text{for } i = 1, 2, \ldots, n \qquad (13)$$

IV. Topological energy functions (TEP)

Energy function is one of the possible Lyapunov functions. The advantage of using energy function in stability analysis is that various terms in it can be given physical interpretation. Particularly with a structure-preserving model for power systems, energy function is the sum of the energy of each individual component of the system. This makes it possible to allocate the aggregate energy to the components of the network. As a result, energy changes during a transient can be decomposed into energy changes in individual power-system elements.

The use of energy function can be related to the equal-areas criterion for one- or two-machine systems. Athay et al.[3] derived an energy function for the reduced system (after

eliminating the load buses) using COA variables. The presence of transfer conductances introduces a path-dependent term. This can be avoided by using the structure-preserving model[6,7]. However, the energy function developed in References 6 and 7 takes account only of constant active power loads and uses absolute rotor velocities in defining the kinetic energy. The latter would be accurate only if an infinite bus were considered in the system.

The development of the energy function given here avoids both the drawbacks mentioned above. Any arbitrary voltage-dependent load characteristics are considered and the COA variables are used.

Consider the energy function defined for the post-fault system

$$W(\theta, \omega, V, \phi, t) = W_1(\omega) + W_2(\theta, V, \phi, t) \qquad (14)$$

where

$$W_1(\omega) = \frac{1}{2} \sum_{i=1}^{m} M_i \omega_i^2$$

$$W_2(\theta, V, \phi, t) = W_{21}(\theta) + W_{22}(t) + W_{23}(V)$$
$$+ W_{24}(V, \theta, \phi) + W_{25}(V, \phi)$$

$$W_{21}(\theta) = \sum_{i=1}^{m} P_{mi}(\theta_i - \theta_{i0})$$

$$W_{22}(t) = \sum_{i=1}^{n} \int_{t_0}^{t} P_{li}(V_i) \frac{d\phi_i}{dt} dt$$

$$W_{23}(V) = \sum_{i=1}^{n} \int_{V_{i0}}^{V_i} \frac{f_{qi}(x_i)}{x_i} dx_i$$

$$W_{24}(V, \theta, \phi) = \sum_{i=1}^{m} [(E_i^2 + V_i^2 - 2E_iV_i \cos(\theta_i - \phi_i))$$
$$- (E_{i0}^2 + V_{i0}^2 - 2E_{i0}V_{i0} \cos(\theta_{i0} - \phi_{i0}))] \frac{1}{2x'_{di}}$$

$$W_{25}(V, \phi) = -\frac{1}{2} \sum_{i=1}^{n} \sum_{j=1}^{n} B_{ij}(V_iV_j \cos\phi_{ij} - V_{i0}V_{j0} \cos\phi_{ij0})$$

W_1 is the kinetic energy and W_2 is the potential energy.

It can be proved, by direct verification, that the system defined by the equations (1)-(13) is conservative.

Proof: Taking partial derivatives of W with respect to V_i, ϕ_i, t, ϕ_i and ω_i respectively, one can easily get (using system equations)

$$\frac{\partial W}{\partial V_i} = \frac{1}{V_i}(Q_{li} + Q_i) = 0, \quad \text{from equation (13)} \qquad (15)$$

$$\frac{\partial W}{\partial \phi_i} = -\frac{E_iV_i \sin(\theta_i - \phi_i)}{x'_{di}} + \sum_{j=1}^{n} B_{ij}V_iV_j \sin\phi_{ij},$$
$$i = 1, 2, \ldots, m$$

$$= \sum_{j=1}^{n} B_{ij}V_iV_j \sin\theta_{ij}, \quad i = m+1, \ldots, n \qquad (16)$$

$$= P_i \quad \text{from equations (8) and (9)}$$

$$\frac{\partial W}{\partial t} = \sum_{i=1}^{n} P_{li} \frac{\partial \phi_i}{dt} \qquad (17)$$

$$\frac{\partial W}{\partial \theta_i} = -P_{mi} + P_{ei} \qquad (18)$$

and

$$\frac{\partial W}{\partial \omega_i} = M_i \omega_i \qquad (19)$$

We have, from equation (12),

$$\sum_{i=1}^{n} \frac{\partial W}{\partial \phi_i} \frac{d\phi_i}{dt} + \frac{\partial W}{\partial t} = \sum_{i=1}^{n} (P_i + P_{li}) \frac{d\phi_i}{dt} = 0 \qquad (20)$$

and

$$\sum_{i=1}^{m} \frac{\partial W}{\partial \omega_i} \frac{d\omega_i}{dt} + \frac{\partial W}{\partial \theta_i} \frac{d\theta_i}{dt} = \sum_{i=1}^{m} (M_i \omega_i - P_{mi} + P_{ei}) \omega_i$$
$$= \sum_{i=1}^{m} \frac{M_i}{M_T} P_{COA} \omega_i = 0, \quad \text{from equation (5)} \qquad (21)$$

Hence,

$$\frac{dW}{dt} = \left[\sum_{i=1}^{m} \frac{\partial W}{\partial \omega_i} \frac{d\omega_i}{dt} + \frac{\partial W}{\partial \theta_i} \frac{d\theta_i}{dt} \right] + \left[\sum_{i=1}^{n} \frac{\partial W}{\partial V_i} \frac{dV_i}{dt} \right]$$
$$+ \left[\sum_{i=1}^{n} \frac{\partial W}{\partial \phi_i} \frac{d\phi_i}{dt} + \frac{\partial W}{\partial t} \right] = 0 \qquad (22)$$

on substituting from equations (15), (20) and (21).

This shows that the total energy of the system is conserved.

Comments

1 It is assumed that the system models are well defined in the sense that the voltages at the load buses can be solved in a continuous manner at any given time during the transient. This means that the system trajectories are smooth and that there are no jumps in the energy function.

2 Consider the term

$$\int_{t_0}^{t} P_{li} \frac{d\phi_i}{dt} dt$$

in the energy function that corresponds to active power component of the load at bus i. Integrating by parts, we get

$$\int_{t_0}^{t} P_{1i} \frac{d\phi_i}{dt} dt$$

$$= \int_{t_0}^{t} f_{pi}(V_i) \, d\phi_i = f_{pi}(V_i) \, \phi_i \Big|_{t_0}^{t}$$

$$- \int_{t_0}^{t} \frac{\partial f_{pi}(V_i)}{\partial V_i} \frac{dV_i}{dt} \phi_i \, dt$$

$$= f_{pi}(V_i) \, \phi_i - f_{pi}(V_{i0}) \, \phi_{i0}$$

$$- \int_{t_0}^{t} \frac{\partial f_{pi}(V_i)}{\partial V_i} \frac{dV_i}{dt} \phi_i \, dt \qquad (23)$$

The second term on the right-hand side of equation (23) is path-dependent. Approximation can be introduced by ignoring this term and evaluating the energy using only the first component, which is path-independent. With this approximation, the energy function (14) can be modified by replacing

$$\int P_{1i} \frac{d\phi}{dt} \quad \text{by} \quad [f_{pi}(V_i) \, \phi_i - f_{pi}(V_{i0}) \, \phi_{i0}]$$

The time derivative of the modified energy function (W_{mod}) will not be zero and given by

$$\frac{dW_{mod}}{dt} = \sum_{i=1}^{n} \frac{\partial}{\partial V_i} f_{pi}(V_i) \frac{dV_i}{dt} \phi_i \qquad (24)$$

With constant voltage or constant active power loads, the right-hand side of equation (24) is zero and the system will be conservative. For other types of load, it is non-zero. However, if the derivative is sufficiently small in magnitude, the use of modified energy function can give an accurate estimation of the stability region.

3   The terms of the energy function can be physically interpreted in the following way[3].

W_1 total change in the rotor kinetic energy relative to COA,

W_{21} change in the potential energy due to mechanical input relative to COA,

W_{22} change in the potential energy due to voltage-dependent active power loads relative to COA,

W_{23} change in the potential energy due to the voltage-dependent reactive power loads,

W_{24} change in the magnetic energy stored in the machine reactances,

W_{25} change in the magnetic energy stored in the transmission lines.

4   The last two terms in the energy function (14) represent the energy in the machine reactances and transmission

line reactances It is shown by Padiyar *et al*[9] that this energy can be expressed as half the sum of reactive power loss in each element of the network (including machine reactances). This energy is thus given by

$$\sum_{k=1}^{n_1} \frac{1}{2} Q_k = \frac{1}{2} \left[\sum_{i=1}^{m} Q_i - \sum_{j=1}^{n} Q_{1j} \right] \qquad (25)$$

where

Q_i reactive power generation (at the internal bus) of generator i

Q_{1j} reactive power load at bus i

n_1 total number of elements in the network including machine reactances.

The right-hand side of equation (25) is easily calculated at the end of power flow solution at each step during the transient. Thus the computation of the overall energy function is simplified.

V. Computation of stability region

Whenever a fault occurs in a power system, the total energy of the post-fault system, whose stability is being examined, increases. After the fault is cleared the total energy is non-increasing. The key idea of the direct method is that the transient stability of the system, for a given contingency, can be determined directly by comparing the gain in the total system energy during the fault-on period with the 'critical' energy. In the past, the critical energy was chosen to be the potential energy at the UEP closest (in terms of energy) to the post-fault equilibrium point. This critical energy usually yields results that are conservative. Recently, the concept of controlling UEP in determining the critical energy has removed much of the conservativeness in the results[3]. Computational simplifications are possible with the use of PEBS method[3,4]

The PEBS method is particularly attractive as it avoids the need for evaluating UEPs. In this method, it is assumed that the critically-cleared trajectory goes near the UEP corresponding to the fault location. PEBS is defined as the surface formed in the angle space by the points corresponding to the first maxima of the potential energy (with respect to UEP). Inside this region, the potential energy increases and in the immediate vicinity outside this region, it decreases. Thus, the instant at which the time derivative of the potential energy function changes its sign from positive to negative can be interpreted to be the instant when the trajectory crosses the PEBS[4]. The value of the potential energy at this time is the critical energy.

The algorithm for the computation of the critical clearing time, T_{cr}, is as follows·

1   Load flow calculation is performed for the pre-fault system to obtain the pre-fault operating point

2   Bus admittance matrix Y_{bus} is formed for the faulted and post-fault networks.

3   Execution of forward numerical integration is initiated for the equations corresponding to the faulted system At the end of each integration interval power flow of the

faulted system is carried out with injected current at the generator buses as inputs. The method of power flow used is taken from Reference 8. Load bus voltages and angles obtained as the output of this load flow are used to evaluate P_{ei} in equation (3) for the next integration step.

4 At the end of each integration interval, using the same input (generator currents) as in Step 3, power flow of the post-fault system is carried out to obtain the bus voltages and angles to be used in the calculation of the energy function.

5 Integration process is continued for the faulted system equations. The values of W, W_2 and $\dot{W}_2$ are monitored for each interval of integration and W_{cr}, critical energy, is obtained as the value of W_2 corresponding to the instant when $\dot{W}_2$ changes its sign from positive to negative. $\dot{W}_2$ is numerically evaluated as

$$\dot{W}_2 = \frac{W_{2(t)} - W_{2(t-1)}}{t} \tag{26}$$

where $W_{2(t)}$ = potential energy at time t, $W_{2(t-1)}$ = potential energy in the previous interval.

6 The critical clearing time (T_{cr}) is obtained as the time when the value of W is equal to W_{cr}.

VI. Numerical examples

VI.1 *Description*
Two examples are considered:

1 4 machine, 6 bus system[10]

2 7 machine, 10 bus system[1]

The single line diagrams with operating data for the above systems are given in Figures 1 and 2. It is assumed that a three-phase fault occurs which is cleared and the line is
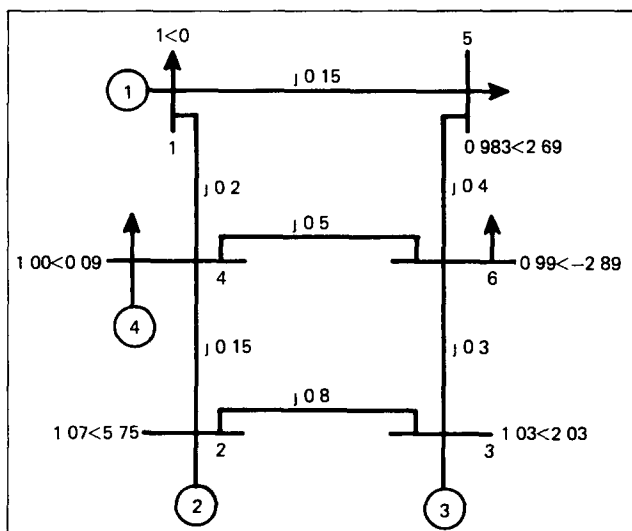

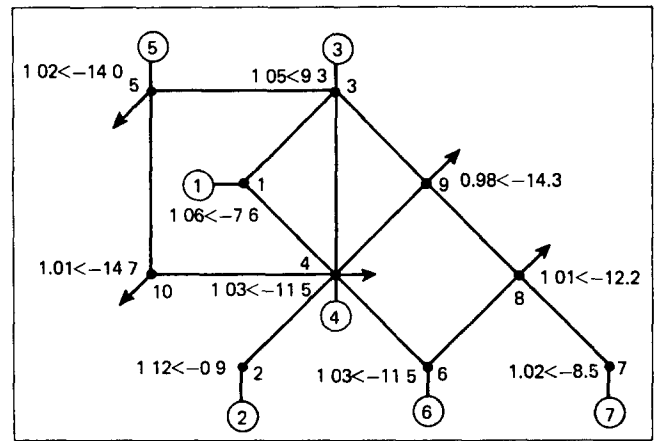Figure 1. Single line diagram of 4-machine system

Figure 2. Single line diagram of 7-machine system

instantaneously reclosed. Thus, the pre-fault and post-fault system configurations are assumed to be same. Different load characteristics are considered. For simplicity, all the loads are assumed to have similar characteristics. The different cases considered for examples 1 and 2 are listed in Tables 1 and 2 respectively. For case (x) in Table 1 and case (v) in Table 2, it is assumed that

$$a_i V_i^2 = b_i V_i = C_i = \tfrac{1}{3}P_{1i}, \quad \text{and} \quad d_i V_i^2 = e_i V_i = f_i = \tfrac{1}{3}Q_{1i}$$

$$\text{for } i = 1, 2, \ldots, n$$

In all cases, T_{cr} is obtained both by prediction by using TEF and digital simulation.

VI.2 *Effect of load model*
Tables 1 and 2 give the T_{cr} obtained by using modified TEF and that obtained by digital simulation for the examples 1 and 2 respectively. It can be observed that the use of TEF results in accurate prediction of T_{cr} in, practically, all the cases considered. It can also be observed that the voltage dependence of active power characteristics has a significant effect on the critical clearing time. It is maximum with constant impedance type of loads, and minimum with the constant power loads and is intermediate with constant current loads. Thus, it may be optimistic to consider the loads to be of constant impedance type. The variation in the reactive power characteristics of loads has no significant effect on T_{cr}. These conclusions may not be valid in all cases but the results bring out the need for accurate load models.

Non-linear characteristics of loads (particularly constant power type) can introduce convergence problems in the network solution during simulation. The non-convergence of the solution implies either the non-existence of the power flow solution or the failure of the solution algorithm.

VI 3 *Constant-impedance type loads*
It is possible to reduce the system network by eliminating load buses for the case of constant-impedance type loads. It is interesting to compare the results obtained on a reduced network with those obtained using a structure-preserving model. The drawback in reducing the network is the creation of transfer conductances (even with lossless lines). Energy function with reduced network W_r and an

Table 1. Critical clearing time for the 4-machine system

Sl. no.	Type of load characteristics	Fault at bus 2 Digital simulation	Fault at bus 2 Energy function method	Fault at bus 3 Digital simulation	Fault at bus 3 Energy function method
1(i)	$K_1V^2+jK_2V^2$	0.430–0.435	0.430–0.435	0.485–0.490	0.485–0.490
1(ii)	$K_1V^2+jK_2V$	0.430–0.435	0.425–0.430	0.480–0.485	0.480–0.485
1(iii)	$K_1V^2+jK_2$	0.430–0.435	0.425–0.430	0.475–0.480	0.475–0.480
1(iv)	$K_1+jK_2V^2$	0.415–0.420	0.415–0.420	0.455–0.460	0.455–0.460
1(v)	K_1+jK_2V	0.420–0.425	0.415–0.420	0.455–0.460	0.455–0.460
1(vi)	K_1+jK_2	0.415–0.420	0.415–0.420	0.455–0.460	0.450–0.455
1(vii)	$K_1V+jK_2V^2$	0.425–0.430	0.420–0.425	0.470–0.475	0.470–0.475
1(viii)	K_1V+jK_2V	0.425–0.430	0.425–0.430	0.475–0.480	0.475–0.480
1(ix)	K_1V+jK_2	0.425–0.430	0.425–0.430	0.470–0.475	0.470–0.475
1(x)	$(aV^2+bV+c)+j(dV^2+eV+f)$	0.425–0.430	0.425–0.430	0.470–0.475	0.470–0.475

Table 2. Critical clearing time for the 7-machine (CIGRE) system

Sl. no.	Type of load characteristics	Fault at bus 1 Digital simulation	Fault at bus 1 Energy function method	Fault at bus 2 Digital simulation	Fault at bus 2 Energy function method	Fault at bus 3 Digital simulation	Fault at bus 3 Energy function method
2(i)	$K_1V^2+jK_2V^2$	0.35–0.36	0.35–0.36	0.35–0.36	0.35–0.36	0.39–0.40	0.39–0.40
2(ii)	$K_1+jK_2V^2$	0.25–0.26	0.25–0.26	0.24–0.25	0.24–0.25	Fails	Fails
2(iii)	K_1V+jK_2	0.33–0.34	0.33–0.34	0.33–0.34	0.33–0.34	Fails	Fails
2(iv)	K_1V+jK_2V	0.31–0.32	0.31–0.32	0.31–0.32	0.31–0.32	0.34–0.35	0.34–0.35
2(v)	$(aV^2+bV+c)+(dV^2+eV+f)$	0.31–0.32	0.31–0.32	0.30–0.31	0.30–0.31	Fails	Fails

Table 3. Effect of transfer conductances on predicted T_{cr}

Faulted bus no.	Reduced system With transfer conductances	Reduced system Without transfer conductances	Structure-preserving model	Digital simulation
2	0.430–0.435	0.44–0.45	0.430–0.435	0.430–0.435
3	0.480–0.485	0.49–0.50	0.485–0.490	0.485–0.490

approximate method for handling transfer conductances given in Reference 3 are used here, for comparison.

Table 3 shows the critical clearing time (T_{cr}) obtained both by digital simulation and prediction for the Example 1 for the following cases:

(a) reduced network, neglecting transfer conductances;

(b) reduced network, considering transfer conductances;

(c) structure-preserving model using TEF.

Table 4 gives similar results for Example 2 except that case (b) is not considered.

It can be observed from Tables 3 and 4 that neglecting the transfer conductances in the function W_r^3 gives a higher

Table 4. Comparison of predicted T_{cr} using reduced system and TEF

Faulted bus no.	Reduced system	Structure-preserving model	Digital simulation
1	0.37–0.38	0.35–0.36	0.35–0.36
2	0.37–0.38	0.35–0.36	0.35–0.36
3	0.41–0.42	0.39–0.40	0.39–0.40

value of T_{cr} than the actual. There is an improvement in considering transfer conductances (see Table 1), but the results are not consistently accurate. The use of structure-preserving model gives consistently accurate results, as the

problem of transfer conductances is avoided. The results show that even for constant-impedance types of load, it is useful to preserve the system structure.

VI.4 Effect of approximation in TEF

The TEF given in equation (14) is modified by ignoring the path-dependent term introduced by voltage-dependent active power loads. In the present analysis modified TEF is used. The time derivative of the modified TEF is given in equation (24) and is non-zero except for the case of constant active power loads. Figure 3 shows the variation of the derivative of modified TEF for the Example 1, case (i)(b) for stable, unstable and sustained fault (at bus 3). It is interesting to observe from this figure that the derivative is zero for most of the transient period considered, in the stable case. Similar variation was also observed for other
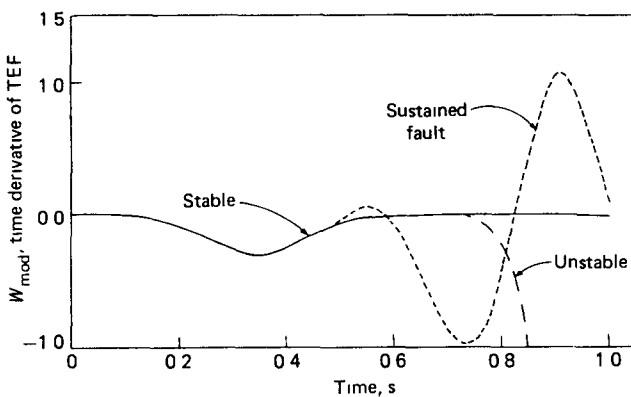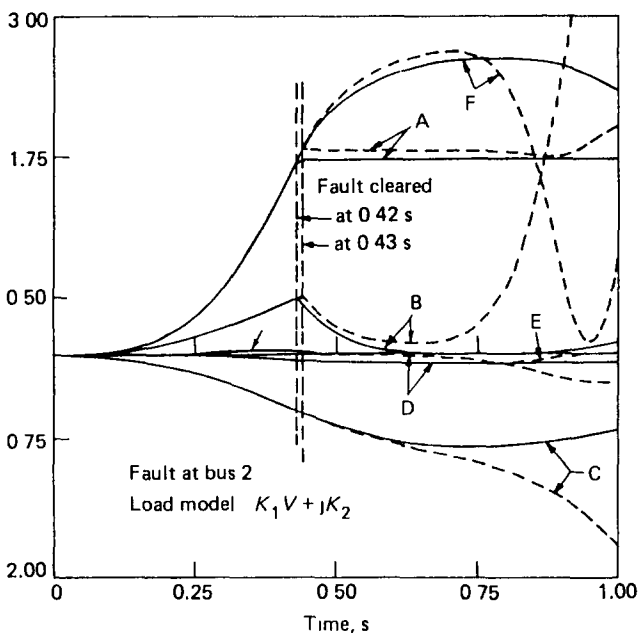

Figure 3. Variation of time derivative of TEF

Figure 4. Variation of TEF and its components. Key:
—— stable case, — — — unstable case. A — total energy,
B — kinetic energy, C — energy due to mechanical inputs,
D — energy due to active power of loads, E — energy due
to reactive power of loads, F — energy due to transmission
elements

load characteristics. Due to this, the predicted values of T_{cr} are accurate, as seen from Tables 3 and 4.

VI.5 Variation of energy function and its components

Figure 4 shows the variation of the various components of modified TEF for the stable and unstable conditions for Example 1, case (ix), and fault at bus 2. The total energy of the system remains almost constant after the fault is cleared, in both the stable and unstable cases.

It can be observed that when the system is stable, the kinetic energy increases until the fault is cleared, and then reduces to zero after some time. This is expected for the first-swing stability and is possible only if the potential energy can increase by an amount equal to the kinetic energy component at the time of clearing[9]. However, it is to be noted that, in general, the kinetic energy contributing to system separation is less than the total kinetic energy[11].

The potential energy terms due to loads contribute very little to the total transient energy. The main contribution is that due to the energy in the transmission lines. The component due to mechanical input decreases and reaches a negative maximum and then increases in the stable case, while it continues to decrease in the unstable case.

VII. Conclusions

In this paper, a topological energy function, based on COA formulation, has been presented with applications. The main feature is the inclusion of voltage-dependent active power loads along with reactive power loads.

The study on two sample systems indicates the following

1 The predicted value of T_{cr} using TEF agrees closely with that obtained by digital simulation in all the cases considered.

2 For constant-impedance types of load, TEF gives better results than those obtained with reduced network. Thus, it is desirable to use a structure-preserving model even for constant-impedance types of load.

3 The effect of voltage-dependent active power loads on the region of stability is quite significant.

4 The modified energy function, ignoring the path-dependent term introduced by non-constant active power loads, appears to give sufficiently accurate results.

VIII. References

1 **Pai, M A** Power System Stability Analysis by Direct Method of Lyapunov North Holland (1981)
2 **Bose Anjan** 'Application of direct methods to transient stability analysis of power systems' Proc. PES Winter Meeting, 1984 Paper 84 WM 070-9
3 **Athay, T, Podmore, R and Virmani, S** 'Practical method for the direct analysis of transient stability' IEEE Trans. Power Appar. & Syst. Vol PAS-98 (March/April 1979) pp 573-584
4 **Kakimoto, N, Ohsawa, Y and Hayashi, M** 'Transient stability analysis of electric power systems via Lure-type Lyapunov function — Parts I and II' Trans. IEE Japan Vol 98 No 5/6 (May/June 1978)
5 **Bergen, A R and Hill, D J** 'A structure preserving model for power system stability analysis' IEEE Trans. Power Appar & Syst. Vol PAS-100 (January 1981) pp 25-35

6   **Narasimha Murthy, N and Musavi, M R** 'A general energy function for transient stability analysis of power systems' *Proc. Mid-West Power Symposium, 1982*

7   **Tsolas, N, Araposthatis, A and Varaiya, P** 'A structure preserving energy function for power system transient stability analysis' Memorandum No UCB/ERL M84/1, Electronics Research Laboratory, University of California, Berkeley (January 1984)

8   **Dommel, H W and Sato, N** 'Fast transient stability solution' *IEEE Trans. Power Appar. & Syst.* Vol PAS-91 (July 1972) pp 1643–1650

9   **Padiya, K R and Varaiya, P** 'A network analogy for power system stability analysis' Preprint (December 1983)

10 **El-Abiad, A H and Nagappan, K** 'Transient-stability regions of multi-machine power systems' *IEEE Trans Power Appar & Syst.* Vol PAS-85 (February 1966) pp 169–179

11 **Fouad, A A and Stanton, S E** 'Transient stability of multi-machine power systems — Part II Critical transient energy' *IEEE Trans. Power Appar. & Syst.* Vol PAS-100 No 7 (July 1981) pp 3417–3424